Topological features of quantum transport in $bi_{1-x}Sb_x$ ($0 \le x \le 0.2$) bicrystals

Cite as: Low Temp. Phys. **49**, 130 (2023); https://doi.org/10.1063/10.0016486
Submitted: 23 November 2022 • Published Online: 25 January 2023

Fiodor Muntyanu, Vitalie Chistol, Elena Condrea, et al.

Low Temperature Physics ARTICLE scitation.org/journal/ltp

Topological features of quantum transport in $bi_{1-x}Sb_x$ ($0 \le x \le 0.2$) bicrystals

Cite as: Fiz. Nizk. Temp. **49**, 139–145 (January 2023); doi: 10.1063/10.0016486
Submitted: 23 November 2022

Fiodor Muntyanu,[1] Vitalie Chistol,[2] Elena Condrea,[1] and Anatolie Sidorenko[1,2,a)]

AFFILIATIONS

[1]Institute of Electronic Engineering and Nanotechnologies, MD 2028 Chisinau, Moldova
[2]Technical University of Moldova, MD 2004 Chisinau, Moldova

[a)]**Author to whom correspondence should be addressed:** Anatoli.sidorenko@kit.edu

ABSTRACT

High-quality $Bi_{1-x}Sb_x$ ($0 \le x \le 0.2$) bicrystals with nanowidth crystallite interfaces (CIs), exhibiting simultaneously superconductivity ($T_c \le 21$ K) and weak ferromagnetism, are studied. A number of unusual features of quantum transport are observed, which are due to topological changes of the Fermi surface of CIs layers, as well as the manifestation of some 3D topological phases of the matter. It is revealed that the flow of Dirac fermions is sensitive to the field orientation, and the localization process occurs only at the $B||$CIs plane. In doing so, the dependences of the Landau level index n on peak position B_n^{-1} at inclination interfaces are extrapolated to -0.5 if $1/B_n \to 0$, as expected for the massless Dirac fermions, while in crystallites and some twisting CIs with an increased degree of imperfection, electronic states are of the Schrodinger type, since n takes integer values. At Sb concentrations of $x \sim 0.04$, the high-field thermomagnetic phenomena of CI layers exhibit behavior of the 3D topological semimetals, whereas in bicrystals with $0.07 \le x \le 0.2$ they manifest typical features of the 3D topological insulators.

INTRODUCTION

It has long been known that the energy spectrum of $Bi_{1-x}Sb_x$ ($0 \le x \le 0.2$) alloys, which is one of the most efficient thermoelectric materials, is significantly rearranged with an increase in the Sb content. Recently, this rearrangement has acquired a special quantum shade associated with the experimental discovery of a first strong 3D Z_2 topological insulator (3D TI) in these alloys.[1,2]

We briefly describe the main changes in the energy spectrum of these extraordinary alloys. In a concentration range of $0 \le x \le 0.07$, the overlap of terms L-T_{45} [see Fig. 1(a)] is gradually removed. At $x \sim 0.04$, an inverted symmetry ordering at L points of the Brillouin zone takes place, a 3D Dirac point is formed,[1] and the massless Dirac fermions appear in quantum transport. In the concentration range of $0.07 \le x \le 0.2$, the overlapping of energetic bands L_a–T_{45} disappears, the T_{45} valence band top descends below the L_a conduction band bottom, the alloys become an inverted band narrow-gap semiconductors, and a topological phase transition from a band insulator to a 3D TI occurs. The $Bi_{1-x}Sb_x$ alloys at $x > 0.22$,[4] due to the overlapping of L_a electron and H hole bands typical for antimony, are expected to be topologically nontrivial semimetals with characteristics of strong 3D TIs. Despite these changes in the carrier energy spectrum of bulk crystalline $Bi_{1-x}Sb_x$ ($0 \le x \le 0.2$), the surface band of the external metallic surface is nearly similar to that of Bi and Sb and consists of one electron pocket at the Γ point and six hole pockets localized on the line between Γ and M points of the Brillouin zone.[1,5]

A very unexpected topological quantum material[6,7] is superconducting crystallite interfaces (CIs) of bismuth- antimony bicrystals. The topology (shape, elongation, volume, etc.) of isoenergetic surfaces of CI layers undergo significant changes depending on the disorientation angles of bicrystals. In some samples, the elongation of the Fermi surface (FS) in interface layers is modified, the FS is rotated in comparison with the ones in crystallites, and the T_{45} hole ellipsoid of revolving turns into a deformed hole pocket with all three main cross-sectional areas of different sizes. The volume of the electron and hole isoenergic pockets of the component layers is considerably higher than that in the isoenergetic surfaces of the respective charge carriers of single-crystalline samples/crystallites.

In the following, we report the high-fields magnetotrans-port anomalies and FS rearrangement in $Bi_{1-x}Sb_x$ ($0 \le x \le 0.2$) bicrystals with nanowidth multilayer interfaces, where sometimes superconductivity is found to occur simultaneously with a weak ferromagnetism. Most of these peculiarities do not stand out in bulk crystalline

samples and are associated with the manifestation of the quantum transport features of Dirac carriers at the bicrystal interfaces.

EXPERIMENTAL TECHNIQUES

Samples for measurements were prepared by the zonal recrystallization method with the application of the double seed technique. They consist of two bulk disoriented crystallites and a nanowidth interface. Two heaters, one to create a molten zone and the other to adjust the temperature gradient among the liquid and solid phases, were used to prepare the samples. Bicrystals of inclination (crystallo-graphic axes of the crystallites are revolved in a single plane at a disorientation angle $\theta \leq 68°$) and twisting types (disorientation angle $\theta_1 \leq 75°$, rotation angle $\theta_2 \leq 10°$) were studied.[6]

Since single-crystalline $Bi_{1-x}Sb_x$ $(0.07 \leq x \leq 0.2)$ are weakly degenerate narrow gap semiconductors with minor impurity residual carrier concentration, the quantum transport at low temperatures does not show well-pronounced oscillations. To use quantum oscillation studies, which is a highly relevant research method, we increased the carriers concentration in the biciystals by lightly doping (≤ 0.01 at.%) with Te (donor type) or Sn impurities (acceptor type). The studies of transport phenomena were performed in transversal ($B_\perp$) or longitudinal ($B_{||}$) magnetic fields [see Figs. 1(b) and 1(c)]. The composition of the samples and the residual concentration of magnetic impurities were monitored using an SEM system, neutron activation analysis, as well as by optical emission spectrometry methods.

The width of interfaces [see Figs. 1(d) and 1(e)] was determined using SEM, from measurements of the superconducting parameters, and also from the transport quantum oscillations.[8] It was revealed that the interfaces consist of a central layer (the width $\sim$ 60 nm) and two similar adjacent (the width $\sim$ 20 nm) layers. The Dingle temperature estimated from quantum oscillations amplitude shows that T_D in crystallites exceeds more than 5 times the value on CIs, confirming their higher structural perfection. Contact electrodes for transport measurements were attached directly on the interfaces by electrospark welding.

The magnetoresistivity $\rho_{ii}(B)$, Hall effect $\rho_{ij}(B)$, and thermomagnetic power $\alpha_{ii}(B)$, including quantum oscillations, were registered in stationary (up to 18 T) and pulse (up to 40 T) magnetic fields.

RESULTS AND DISCUSSION

Galvanomagnetic quantum transport

New qualitative advantages have been unveiled by research in high magnetic fields, especially in the area of manifestation of quantum oscillations $\rho_{ij}(B)$ arising from periodic changes in the thermodynamic potential and in the probability of electron scattering on the FS. These studies involve the detection of possible transitions to a collective state with exceptional quantum properties, leading to the discovery of new three-dimensional topological features.

To reveal the most relevant high-field peculiarities of magnetoresistance and longitudinal Hall effect [measured in longitudinal geometry: magnetic field B is parallel to the Hall voltage U, yet both are perpendicular to the current I, see Figs. 1(b) and 1(c)], representing different Dirac band signatures, we will examine the results obtained in $Bi_{1-x}Sb_x$ bicrystals with nanowidth CIs.

Figure 2(a) shows typical examples of quantum oscillations of both longitudinal Hall effect (LHE) and magneto- resistance of inclination and twisting bicrystals, exhibiting for various samples one ($T_c \sim 3.1$–3.8 K) or two ($T_{c1} \sim 8.3$–21 K, $T_{c2} \sim 3.7$–4.6 K) transitions in superconducting state and magnetic hysteresis loops like for strong type-II superconductors, ferromagnetic loops on paramagnetic background or dual features — superconducting and ferromagnetic.[6] It turned out that the oscillations spectrum contains frequencies from the FS of crystallites and interfaces. Similar to Bi bicrystals,[6] a number of longitudinal Hall quasi-plateaus [see Fig. 2(a), curves 4, 5], along with minima in magneto-resistance, have also been observed in inclination $Bi_{1-x}Sb_x$ $(x \leq 0.06)$ bicrystals with n-type conductivity and at a disorientation angle of $\theta \leq 9°$, having a lower level of disorder and dislocation density ($T_D \leq 1$ K). In single crystals/crystallites, as well as in bicrystals with an

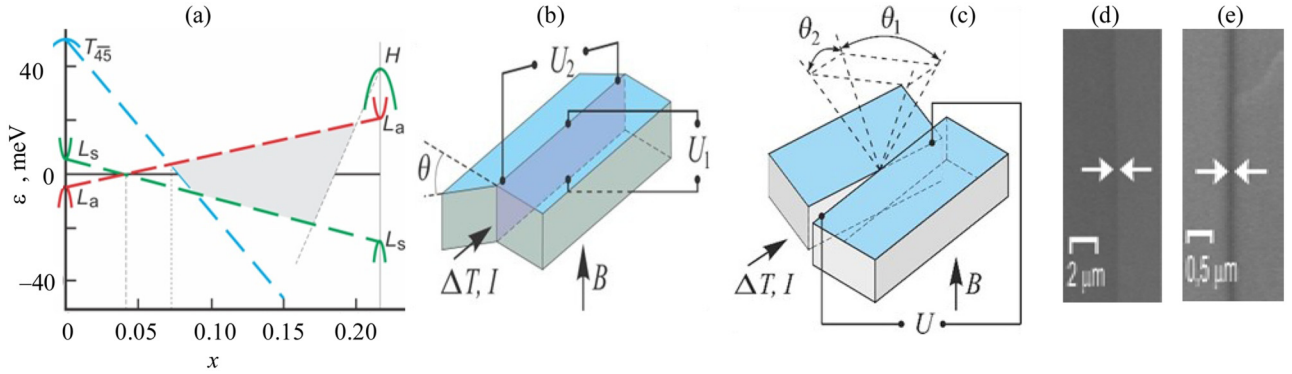

FIG. 1. (a) Diagram of the energy bands rearrangement near Fermi level in dependence of Sb concentration x in single crystals of $Bi_{1-x}Sb_x$ alloys. Schematic of measuring the quantum transport in inclination (b) and twisting (c) bicrystals. (d), (e) SEM images of $Bi_{0.93}Sb_{0.07}$ and $Bi_{0.85}Sb_{0.15}$ bicrystals with n- and p-type conductivity, respectively. The arrows indicate the CI location.

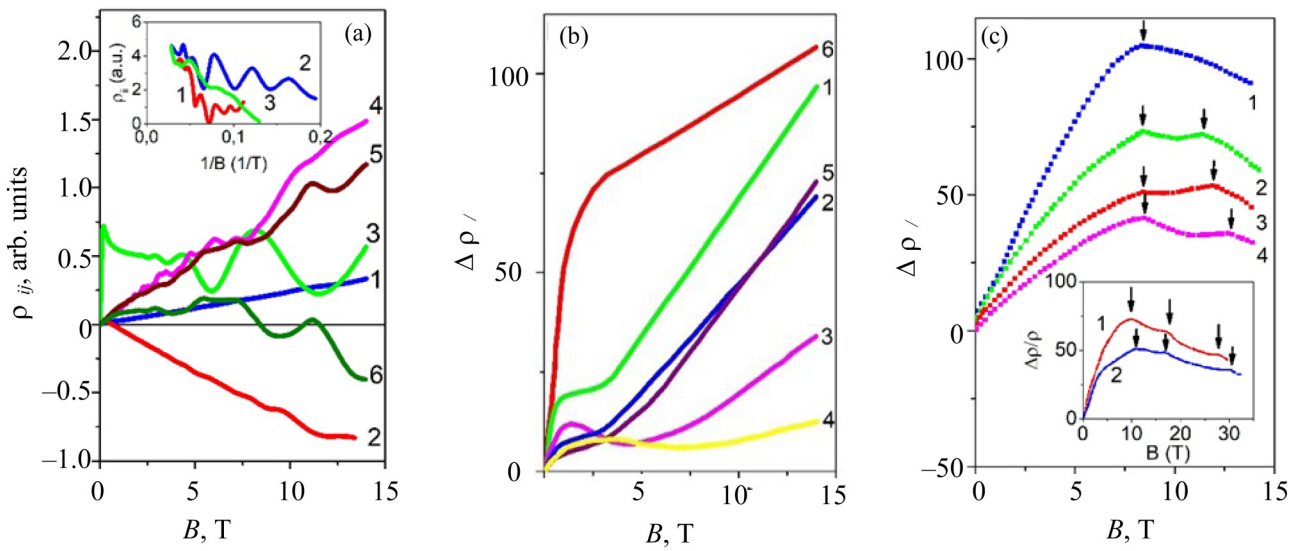

FIG. 2. High-field dependences of magnetoresistivity $\rho_{ij}(B)$ and longitudinal Hall resistivity $\rho_{ij}(B)$ in $Bi_{1-x}Sb_x$ ($0 \le x \le 0.2$) bicrystals. (a) $\rho_{ij}(B)$, $x = 0.12$, 4.2 K, B^+ (*1*), B^- (*2*), $\theta_1 = 12°$, $\theta_2 = 2°$; (*3*) $\rho_{ii}(B)$, $x = 0.07$, $\theta = 68°$, 2.1 K; (*4*) $\rho_{ij}(B)$, $x = 0.06$, $\theta = 9°$, 4.2 K, scale for $\rho_{ii}(B)$ 1:1.5; (5) $\rho_{ij}(B)$, $x = 0.05$, $\theta = 7°$, 2.1 K, scale for $\rho_{ii}(B)$ 1:1.3; (6) $\rho_{ij}(B)$, $x = 015$, $\theta = 16°$, 4.2 K; (*4*)–(*6*) *n*-type conductivity; (*1*)–(*3*) *p*-type conductivity; (*3*)–(*6*) inclination bicrystals, (*1*), (*2*) twisting bicrystals; Inset: (*1*) $\rho_{ii}(B)$, $x = 0.15$, $\theta_1 = 15°$, $\theta_2 = 3°$; (*2*) $\rho_{ii}(B)$, $x = 0.12$, $\theta_1 = 12°$, $\theta_2 = 2°$; (*3*) $\rho_{ii}(B)$, $x = 0.07$, $\theta_1 = 19°$, $\theta_2 = 2°$; (1)–(3) twisting bicrystals of *n*-type conductivity; (*1*)–(*3*) pulsed magnetic fields (up to 40 T); (b) (*1*) $\rho_{ii}(B)$, $x = 15$, $\theta = 13°$, 77 K; (6) $\rho_{ii}(B)$, $x = 15$, $\theta = 15°$, 77 K; (3) $\rho_{ii}(B)$, $Bi_{0.93}Sb_{0.07}$, 77 K; (6) $\rho_{ii}(B)$, $Bi_{0.93}Sb_{0.07}$, 77 K, $\theta = 6°$; (*3*) $\rho_{ii}(B)$, $Bi_{0.82}Sb_{0.18}$, 77 K; (*4*) $\rho_{ii}(B)$, $Bi_{0.82}Sb_{0.18}$, 77 K, $\theta = 16°$, (*3*), (*5*) single crystals, (*1*), (*2*), (*4*), (*6*) bicrystals, (*3*)–(*6*) *n*-type conductivity. Magnetic field is oriented perpendicular to the CI plane near the C_2 axis of crystallites; (c) (*1*) single crystal, $x = 0.08$; (*2*), (*3*), and (*4*) twisting bicrystals: (*2*) $x = 0.08$, $\theta_1 = 4°$, $\theta_2 = 2°$; (*3*) $x = 0.09$, $\theta_1 = 9°$, $\theta_2 = 4°$, (*4*) $x = 0.08$, $\theta_1 = 9°$, $\theta_2 = 2°$. Arrows indicate the magnetic fields at which the semiconductor-semimetal transition takes place; (a), (c) Magnetic field is oriented along the CI plane near the C_3 axis of crystallites. Inset: (*1*) $x = 0.08$, $\theta_1 = 4°$, $\theta_2 = 2°$, 4.2 K, (*2*) $x = 0.09$, $\theta_1 = 12°$, $\theta_2 = 2°$, 4.2 K, (*1*), (*2*) twisting bicrystals.

increased degree of inhomogeneity [higher Sb content, doped with Sn acceptor impurity, a higher degree of imperfection ($T_D \ge 4$ K), larger disorientation angles, etc.], such peculiarities do not appear. Therefore, we concluded that the Hall plateaus are directly related to the Dirac electrons of the interfaces. It was also found that the Hall plateaus vanish by magnetic field reverse, thereby indicating that the flow of Dirac fermions is sensitive to the field direction and that the localization process runs only in the magnetic field oriented along the CI plane. This suggests that the backscattering of carriers in the quantum Hall state is suppressed at the bicrystal interfaces but can be restored by the static disorder of multiple scattering processes.[1–3] The disappearance of Hall plateaus at CIs with nontrivial topology of the band structure and an increased level of disorder results in a finite transport length, restricting quasi-ballistic transport[2,3] to nanowidth $Bi_{1-x}Sb_x$ ($x \ge 0.07$) interfaces.

An important feature of LHE, which is associated with the presence of different Dirac electrons in crystallites and interface layers, is the observation of the Umkehr effect/commutation effect (dependence of transport effects values on reversal magnetic field). Note that, at $B_{||}C_3$, the crystal symmetry inhibits the occurrence of the Umkehr effect in rhombohedral single-crystalline bismuth-antimony. Nevertheless, it is clearly manifested in bicrystals [see Fig. 1(a), curves *1, 2*] at $B||$CIs plane (near C_3 axes of crystallites). At that, the quantum oscillations frequencies remain the same, but their amplitude changes significantly and the shifts of the phase take place if the direction of the magnetic field is switched. This means that, for a given field orientation, the main axes of the isoenergetic surfaces of CI carriers due to topological changes of FS do not coincide with the crystallographic axes of crystallites and at least two types of carriers with different localization in k- space are involved in the charge transfer.

It was also found that, at $B||$CIs, the quantum oscillations of magnetoresistance and the Hall effect [see Fig. 2(a)] contain, along with the frequencies associated with the FS of crystallite, two new frequencies connected with FS cross-sections of the CIs carriers. These oscillations are developed separately in the magnetic field of $B \le 40$ T, and their spectrum is composed of one or two frequencies only (manifested at different values of the magnetic field),[6–8] which can be simply determined graphically from the linear dependences of the Landau level index n on the B_n^{-1} position of the oscillation peaks. The oscillations frequencies for crystallite find their explanation in the one-particle picture,[9] while the other two harmonics, observed from 2–2.5 and 10–11 T, exclusively belong to the central and adjacent layers of the interfaces. Moreover, new harmonics appear in almost all bismuth-antimony bicrystals, regardless of the composition, type of doping, disorientation of crystallites, etc. The beginning of the manifestation of new galvanomagnetic quantum oscillations characterizes almost the same thickness of nanolayers for bismuth, antimony, and bismuth-antimony alloys. Important parameters extracted from quantum oscillations

are the cyclotron mass m/m_e (m_e is the free-electron mass) of carriers for crystallites and the adjacent and central layers of CIs, which in $Bi_{1-x}Sb_x$ ($0 \le x \le 0.2$) roughly corresponds to a ratio (in m/m_e units of crystallite carriers) 1:2:5; this fact shows that the electron mass in CI layers is a few times higher than the respective value in crystallites.

Unusual $\Delta\rho/\rho$ dependences on the magnetic field and disorientation angle θ were registered [see Fig. 2(b)] in $Bi_{1-x}Sb_x$ ($0.07 \le x \le 0.2$) inclination *n*-type bicrystals. For instance, in single crystals at $B \perp C_2$ and bicrystals at B⊥CIs, after quadratic growth in weak fields at $T > 20$ K,[10] $\Delta\rho/\rho$ undergoes saturation or slightly decreases and then linearly increases $\sim B$ in high magnetic fields. In addition, in bicrystals up to disorientation angle $\theta \approx 7°$, the plateau broadens; however, further, at $\theta > 18°$, it disappears as the Fermi level moves away from topological peculiarity. The observed features of $\Delta\rho(B)/\rho$ clearly indicate the manifestation of a small group of infinitely moving electrons arising from a "temperature breakdown"[10] and the emergence of a new type of symmetry on CIs associated with the Fermi surface rotation.[8]

Another remarkable feature in magnetic fields is observed in pure $Bi_{1-x}Sb_x$ ($0.08 \le x \le 0.15$) bicrystals beyond the quantum limit (QL), where the charge carriers occupy only the lowest Landau level ($j = 0$) and the band edge displacement takes place $\Delta\varepsilon = 1/2\hbar\omega(1-\Delta\varepsilon_s/\Delta\varepsilon_0)$ depending on the ratio of spin $\Delta\varepsilon_s$ and orbital $\Delta\varepsilon_0$ level splitting. Figure 2(c) shows field dependences of magnetoresistance $\Delta\rho/\rho$ in a single crystal and twisting small disorientation angle (SDA) bicrystals. In a magnetic field oriented along the CIs plane, up to 2 T, regular Shubnikov-de Haas oscillations are detected. The first maximum at $B \sim 8.5$ T in the $\Delta\rho(B)/\rho$ dependences for SDA biciystals (curves *2*, *3*) is registered at the same field as for the single crystals (curve *1*); this fact suggests that a semiconductor-semimetal transition is induced in crystallites.[11,12] For higher magnetic fields, second (≈11 T) and third (≈25 T) additional maxima were revealed; the occurrence of these maxima obviously represents a semiconductor-semimetal transition in the adjacent and central layers of interfaces. Both maxima (second and third) occur at different field values for the bicrystals with various disorientation angles. Note that the transitions appear also at quite different values of *B*; therefore, the cyclotron mass of the relevant charge carriers and the $\Delta\varepsilon_s/\Delta\varepsilon_o$ ratio in crystallites and in the CI region of the SDA bicrystals should differ considerably. This implies a significant increase in the spin-orbit interaction at the interfaces and the existence of gapless electronic states at the bicrystal boundary.

Thus, the galvanomagnetic study in quantizing magnetic fields shows that the features of the coexistence of superconductivity and weak ferromagnetism in 3D TI interfaces preponderantly is due to the fact that the flow of Dirac electrons depends on the magnetic field direction. In doing so, a new type of symmetry arises at the rotation of the isoenergetic surfaces of carriers, the topology of the FS changes significantly with an increase in the crystallite disorientation angle, the enhancement of spin-orbit interaction takes place, there appear the gapless electronic states at the crystallite interfaces and several groups of electrons with different effective masses participate in quantum transport, etc.

Thermomagnetic quantum transport

A study of thermomagnetic phenomena in quantizing magnetic fields provides a possibility of revealing the Dirac band signature, factors combining entropy with charge transport, features of the novel ground state, exotic electronic order, and — why not — finding out new possibilities for device applications, based on exotic thermomagnetic characteristics.[13–15]

Note that the thermomagnetic effects of anisotropic semimetals and narrow gap semiconductors, as well as some other transport phenomena, consist of two — even and odd — components leading to the manifestation of an Umkehr effect on reversal

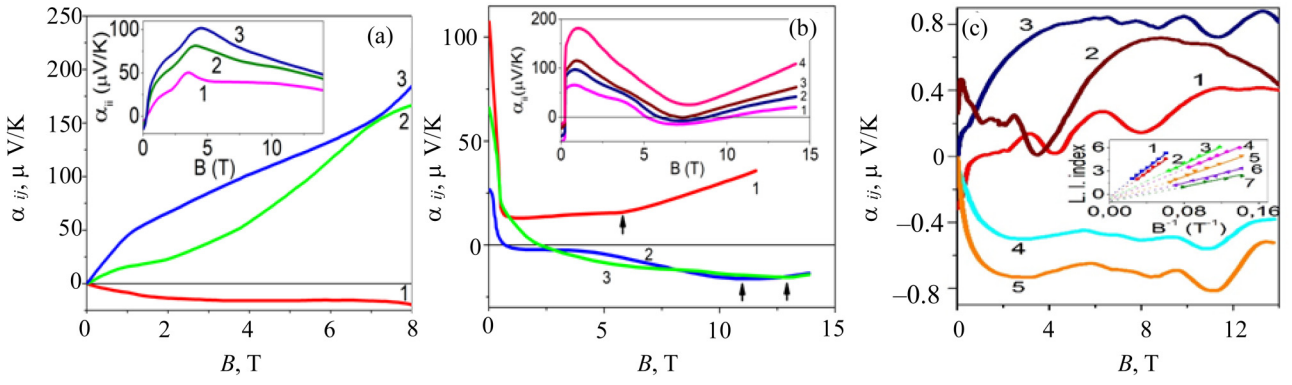

FIG. 3. High-field dependences o(B) for single undoped crystals (a), (b) and $Bi_{1-x}Sb_x$ ($0 \le x \le 0.2$) biciystals (c) with n- orp-type conductivity. (a) $B_{||}C_2$, (1) Bi, 4.5 K, (*2*) $x = 0.03$, 4.5 K, (*3*) $x = 0.05$, 4.5 K; Inset: $B_{||}C_3$, $x = 0.03$, (*1*) 4.8 K, (*2*) 5.3 K, (*3*) 6 K; (*b*) $B_{||}C_3$, (*1*) $x = 0.08$, 8.8 K, (*2*) $x = 0.09$, 10 K, (*3*) $x = 0.1$, 6.3 K. The arrows indicate the critical magnetic field of the semiconductor-semimetal transition; Inset: (*1*) $x = 0.07$: 4.6 K, (*2*) 4.8 K, (*3*) 5.1 K, (*4*) 5.5 K; (c) Δ||*U*, *B*|| CIplane: (*1*) $\theta = 8°$, 8.6 K, $x = 0.04$, (*2*) $\theta = 8°$, 7.6 K, $x = 0.04$, (*3*) $\theta = 7°$, 4.25 K, Bi, (*4*) $\theta = 8°$, 6.7 K, $x = 0.11$, (*5*) $\theta = 4°$, 6.8 K, $x = 0.09$; Inset: The quantum oscillation peaks position B_n^{-1} versus Landau level index *n* for CIs layers of $Bi_{1-x}Sb_x$ bicrystals: (*1*) $x = 0.07$, $\theta = 68°$, (*2*) $x = 0.15$, $\theta_1 = 15°$, $\theta_2 = 3°$, (*3*) $x = 0.04$, $\theta = 8°$, (*4*) $x = 0.06$, $\theta = 9°$, (*5*) $\theta = 0.07$, $\theta = 68°$, (*6*) $x = 0.07$, $\theta = 5°$, (*7*) $x = 0.15$, $\theta_1 = 15°$, $\theta_2 = 3°$, (*2–4*, *6*, *7*) n-type bicrystals, (*1*, *5*) p-type bicrystals.

magnetic field. Moreover, at low temperatures, a considerable contribution to thermo-magnetic power comes from the effect of phonon drag of charge carriers, which sometimes significantly exceed the diffusion component.

Figure 3(a) shows that the odd component of thermomagnetic power $\alpha_{ii}(B)$ at $B_{||}C_2$ in bulk single crystalline $Bi_{1-x}Sb_x$ ($0 \le x \le 0.06$) exceeds the positive even part, despite that the overlap of the L_s-T_{45} bands gradually decreases with growing in Sb content. An increase in the phase volume of phonons interacting with charge carriers in quantizing magnetic fields makes the phonon drag component $\alpha_{ii}(B)$ much larger than the diffusion part and compensates for the fluctuations in the carrier concentration. The insets of Figs. 3(a) and 3(b) show that, at $T < 5$ K, in $Bi_{1-x}Sb_x$ ($x < 0.04$) single crystals on $B_{||}C_3$ beyond the quantum limit, $\alpha_{ii}(B)$ sharply decreases.

In addition, $\alpha_{ii}(B)$ reaches the minimum value, changes the sign even in p-type samples, and grows almost linearly in a magnetic field; this finding is attributed to a rapid increase in the lowest Landau level degeneracy and also the hole concentration beyond QL. The change in the sign of the thermomagnetic power in strong magnetic fields is associated with the predominant interaction of charge carriers with phonons, which leads to the effect of phonon drag of carriers in the opposite direction of motion (U transfer processes). However, after inversion of L_s/L_a terms and forming of Dirac point, the thermomagnetic power of bulk crystalline $Bi_{1-x}Sb_x$ ($0.08 \le x \le 0.15$) has a minimum [see Fig. 3(b)] associated with the semiconductor-semimetal transition in an ultra-quantum magnetic field.[11,12] At the transition in semimetallic state $\alpha_{ii}(B) \approx B^{-0.5}T^{1.5}$, due to the increase in the carrier concentration and changes in their relaxation mechanisms.

Figure 3(c) shows examples of $\alpha_{ii}(B)$ dependences at B||CIs in $Bi_{1-x}Sb_x$ ($0.04 \le x \le 0.12$) bicrystals with n- and p-types conductivity. The results for bicrystals differ significantly from those obtained in pure and doped single crystals, especially since thermomagnetic power is much higher (at least twice) due to the high conductivity of the constituent layers of nanowidth interfaces, an increase in the number of phonons interacting with carriers, and also with a weak imbalance in the concentration of electrons and holes under conditions of the phonon drag effect.

As we recently found,[16] $\alpha_{ii}(B)$ of bicrystals with Sb concentrations $x \approx 0.04$ exhibits a feature of 3D topological semimetals[17–19] — a linear increase in magnetic field without saturation and a sign change beyond the quantum limit of charge carriers. On the contrary, in bicrystals with a higher Sb content ($0.07 \le x \le 0.12$), the monotonic part of the $\alpha_{ii}(B)$ dependences reaches saturation or gradually increases, which is typical for 3D TI. So, the $Bi_{1-x}Sb_x$ ($0.04 \le x \le 0.12$) biciystals may open up promising prospects for a detailed study of topological phase transitions[19–21] from a 3D topological semimetal to a 3D topological insulator and can make a significant contribution to the development of new electronic devices.[22–24]

The spectrum of $au(B)$ quantum oscillations of the $Bi_{1-x}Sb_x$ ($0.04 \le x \le 0.12$) bicrystals with n-and p-types conductivity, just like other transport phenomena, contains frequencies for crystallites and two new harmonics belonging to CIs adjacent and central layers [see Fig. 3(c)]. In magnetic fields directed along C_3 axes (CIs plane) was detected a single frequency of the quantum oscillations for crystallites, which characterize the electronic states of the Schrodinger type,[16] since $n(1/B_n)$ takes an integer value. On the other hand, in fields higher than 2.5 T, two $\alpha_{ii}(B)$ harmonics with frequencies about 2 and 5 times exceeding those of crystallites, were recorded. To specify the type of CIs electrons in inclination and twisting bicrystals, we analyzed in detail the dependences $n(1/B_n)$ for the central and adjacent layers. It has been found that in inclination bicrystals in both cases $n(1/B_n)$ takes values close -0.5 if $1/B_n \to 0$, as should be expected for the massless Dirac fermions, while in twisting bicrystals with more imperfection ($3.5\ \text{K} \le T_D \le 9$ K) the interface electronic states are of the Schrodinger type, since n takes integer values.[6] The nontrivial π−Berry phase observed in the $\alpha_{ii}(B)$ and $\rho_{ii}(B)$ quantum oscillations [see Fig. 3(c), inset] of CIs layers (central and adjacent), convincingly confirm the 3D topological phase manifestation at the entire bicrystal interface.

So, it turned out that the thermomagnetic power of bicrystals significantly surpasses that of single crystals/crystallites; the spectrum of $\alpha_{ii}(B)$ quantum oscillations of bicrystals contains frequencies for crystallites and two new harmonics belonging to CIs adjacent and central layers; the thermomagnetic power of bicrystals, where the Dirac point is formed, exhibits feature of 3D topological semimetals, while in bicrystals with a higher Sb content the properties of a 3D topological insulator are clearly manifested.

CONCLUSIONS

The quantum transport in bicrystals of 3D topological insulators $Bi_{1-x}Sb_x$ ($0 \le x \le 0.2$) related to the interface Dirac electrons is studied. Unusual topological features related to the interface Dirac electrons have been revealed: the longitudinal Hall quasi-plateaus together with minima in magnetoresistance; the manifestation of the Umkehr effect, not allowed by the crystal symmetry; two new harmonics of quantum transport from interface layers, which are pertinent to areas larger than cross-sectional areas of the FS of crystallites; the magnetoresistance peculiarities, indicating both the occurrence of a small group of the infinitely moving electrons and the electronic phase transitions of the semiconductor-semimetal type in magnetic field. In bulk anisotropic single crystals of $Bi_{1-x}Sb_x$ ($0 \le x \le 0.2$) alloys of A7-type rhombohedral structure such unexpected features do not occur under normal ambient conditions. Consequently, in order to detect the above-mentioned features of quantum transport phenomena in other A7-type rhombohedral structures,[25] a certain type of structural deformation with a modification of the FS of charge carriers is required. It is also necessary to limit quasi-ballistic transport to nanoscale to enhance the spin-orbit interaction and the interaction of Dirac carriers with structural defects.

ACKNOWLEDGMENTS

The authors are sincerely grateful to prof. V. Nizhan-kovskii and A. Gilewski for their support in measuring the transport phenomena in high magnetic fields. The work is done in framework of the project RSF Nr. 20-62-47009 “Physical and engineering basis of computers non von Neumann architecture based on superconducting spintronics” (the article conceptualization, methodology and software elaboration) and the project of ANCD foundation no. 20.80009.5007.11, titled “Nanostructuri si nano-materiale functionale pentru industrie si agricultura” (technology of the crystals

growth elaboration, samples fabrication, magnetotransport measurements).

REFERENCES

[1]Jeffrey C. Y. Teo, Lag Fu, and C. L. Kane, Phys. Rev. B **78**, 045426 (2008).
[2]D. Hsieh, D. Qian, I. Wray, Y. Xia, Y. Hor, R. J. Cava, and M. Z. Hasan, Nature (London) **452**, 970 (2008).
[3]Jn H. Bardarson and Je E. Moore, Rep. Prog. Phys. **76**, 056501 (2013).
[4]F. M. Muntyanu, V. G. Kistol, and I. A. Popov, Phys. Status Solidi (b) **148**, K37 (1988).
[5]M. Bianchi, D. Guan, A. Strozecka, C. H. Voetmann, S. Bao, J. I. Pascual, and A. Eiguren, and P. Hofman, Phys. Rev. B **85**, 155431 (2012).
[6]F. M. Muntyanu, A. Gilewski, A. J. Zaleski, V. Chistol, V. Munteanu, K. Rogacki, and A. Sidorenko, *Functional Nanostructures and Metamaterials for Superconducting Spintronics* (Springer International Publishing AG, 2018), Chap. 12, p. 247.
[7]F. M. Muntyanu, A. Gilewski, K. Nenkov, J. Warchulska, and A. Zaleski, Phys. Rev. B **73**, 132507 (2006).
[8]F. M. Muntyanu, A. Gilewski, K. Nenkov, A. Zaleski, and V. Chistol, Phys. Rev. B **76**, 014532 (2007).
[9]A. A. Taskin and Y. Ando, Phys. Rev. B **80**, 085303 (2009).
[10]F. M. Muntyanu and G. S. Gudima, Solid State Physics **36**, 3155 (1994).
[11]E. W. Fenton and J.-P. Jan, and Å. Karlsson, J. Low Temp. Phys. **3**, 147 (1970).
[12]N. B. Brandt, Ya. G. Ponomarev, and S. M. Chudinov, J. Low Temp. Phys. **8**, 369 (1972).
[13]T. Yamashita, Y. Shimoyama, Y. Haga, and T. D. Matsuda, E. Yamamoto Y. Onuki, S. Fujimoto, A. Levchenko, T. Shibauchi, and Y. Matsuda, Nat. Phys. **11**, 17 (2015).
[14]R. Bel, K. Behnia, Y. Nakajima, K. Izawa, Y. Matsuda, H. Shishido, R. Settai, and Y. Onuki, Phys. Rev. Lett. **92**, 217002 (2004).
[15]N. P. Armitage, E. J. Mele, and Ahi Vishwanath, Rev. Mod. Phys. **90**, 015001 (2018).
[16]F. M. Muntyanu and V. Chistol, Physica B Condens. Matter **568**, 66 (2019).
[17]X. G. Wan, A. M. Turner, A. Vishwanath, and S. Y. Savrasov, Phys. Rev. B **83**, 205101 (2011).
[18]S. M. Young, S. Zaheer, J. C. Y. Teo, C. K. Kane, E. J. Mele, and A. M. Rappe, Phys. Rev. Lett. **108**, 140405 (2012).
[19]Z. J. Wang, H. M. Weng, Q. S. Wu, X. Dai, and Z. Fang, Phys. Rev. B **88**, 125427 (2013).
[20]A. A. Burkov, Nat. Mater. **15**, 1145 (2016).
[21]F. M. Muntyanu, A. Gilewski, A. J. Zaleski, V. Chistol, and K. Rogacki, Phys. Lett. A **381**, 2040 (2017).
[22]M. G. Blamire and J. W. A. Robinson, J. Phys. Condens. Matter **26**, 453201 (2014).
[23]J. J. Urban, A. K. Menon, Z. Tian, A. Jain, and K. Hippalgaonkar, J. Appl. Phys. **125**, 180902 (2019).
[24]H.-J. Kim, K.-S. Kim, J.-F. Wang, M. Sasaki, N. Satoh, A. Ohnishi, M. Kitaura, M. Yang, and L. Li, Phys. Rev. Lett. **11**, 246603 (2013).
[25]Y. Shu, D. Yu, W. Hu, Y. Wang, G. Shen, Y. Kono, B. Xu, J. He, Z. Liu, and Y. Tian, PNAS **114**, 3375 (2017).